Journal of Statistical Physics, Vol. 74, Nos. 1/2, 1994

Ensemble Properties and Molecular Dynamics of Unstable Systems

O. Bokhove,[1] C. Bruin,[2] and A. Compagner[2]

Received October 15, 1992; final August 31, 1993

The Hertel–Thirring cell model for unstable systems (of purely attractive particles) is solved in the canonical ensemble for arbitrary dimensions. The differences between the phase transitions found in the canonical and in the microcanonical ensemble are discussed. The cluster phase (with a complete collapse in the ground state) exhibits the nonextensive character of the cell model. The results of the cell model are compared with molecular-dynamics simulations of a one-dimensional model with a rectangular-well pair potential. The simulations support the relevance of the cell model to characterize basic properties of gravitational systems.

KEY WORDS: Cell model; thermodynamic limits; nonextensivity; MD simulations; collapsing systems.

1. INTRODUCTION

The statistical mechanics and molecular dynamics of systems with Newtonian gravitational interaction between particles are complicated by the long range, the singularity at the origin, and the purely attractive character of the gravitational potential. These properties give rise to a violation of the usual stability or extensivity condition, which is valid for short-range potentials with a sufficiently strong repulsion at small interparticle distances (such as the Lennard-Jones potential). Models for finite systems of particles with nonsingular purely attractive potentials have been found to exhibit two phases: one with a homogeneous distribution of the particles in space and one with a single cluster floating in a homogeneous background and containing a considerable number of particles. This was found by Hertel

[1] Department of Physics, University of Toronto, Toronto M5S 1A7, Ontario, Canada.
[2] Laboratory of Applied Physics, 2600 GA, Delft, The Netherlands.

0022-4715/94/0100-0055$07.00/0

and Thirring[1] in the cell model for three dimensions in the canonical and microcanonical ensembles, by Compagner *et al.*[2] in the cell model for arbitrary dimensions in the microcanonical ensemble, and for a general purely attractive gravitational potential in the canonical ensemble by Kiessling.[3] In the cell model the volume is divided into hypercubic cells of equal size and two particles contribute a negative amount $-\varepsilon$ to the potential energy if and only if they are in the same cell. As opposed to stable models, it was found that the cell model in the microcanonical ensemble has a negative specific heat for a certain range of energies. In this paper we investigate the phase transition in two different asymptotic limits and compare the solutions in the canonical and in the microcanonical ensemble in arbitrary dimensions. The main result is the analogy between the statistical mechanical behavior of unstable systems and the occurrence of clusters in cosmology. This analogy is remarkable, since it is based only on the crudest approximation of the gravitational potential. The metastable region between the homogeneous and the cluster phase in the microcanonical ensemble turns out to be the most interesting part of the phase diagram, as was stated in ref. 2 and exemplified in the study of perturbed unstable systems by Posch *et al.*[4]

The shortcomings of the artificial space dependence of the potential in the cell model have been investigated with molecular-dynamics simulations in two dimensions by Compagner *et al.*[2] In these simulations, the pair potential used was

$$\phi(r) = -\varepsilon \exp(-r^{\delta}/\sigma^{\delta}) \tag{1}$$

where r is the distance between two particles, ε the depth of the potential, σ the range of the potential, and δ an even positive integer. Note that only the purely attractive character of the gravitational potential has remained. To compare the simulations with the cell model, a relation between σ and the cell size must be adopted. In ref. 2 a crude estimate of the right order of magnitude was found by putting the cell size equal to twice the value of r at the inflection point of Eq. (1). With this identification, a good qualitative agreement between cell model and simulations is found. Similar simulations were carried out by Posch *et al.*[5]

To see whether it would improve the agreement, a model with a rectangular well of depth ε and range σ, the case $\delta \to \infty$ in Eq. (1), is studied and compared with the cell model. The discrete character of the pair potential then resembles the discrete form of the potential in the cell model better than the smooth potential for small values of δ. The simulations reported here are restricted to the one-dimensional case. Due to the absence of a hard core in Eq. (1) the dependence on the dimension of the system is expected to be rather weak. It should be noted that the pair potential in

Eq. (1) does not depend on the dimension and is not meant to mimic in any sense a genuine one-dimensional gravitational potential, obeying the Poisson equation. Unfortunately, the reduction to one dimension did not result in the expected decrease of relaxation times. The advantage of improved numerical efficiency is apparently shattered by the restriction of the kinetic degrees of freedom to only one dimension.

The motivation for the present study lies in the following questions: (1) Does the usual formalism of statistical mechanics still lead to sensible thermodynamic results even when the stability condition does not hold? (2) Does statistical mechanics provide a general background for the discussion of cosmological problems?

2. THE CELL MODEL IN THE CANONICAL ENSEMBLE

We sketch the solution of the cell model in the canonical ensemble, referring to the earlier paper[2] for mathematical details and emphasizing the differences with the derivation in the microcanonical ensemble. The hypervolume $V = ML^d$ in d dimensions contains N particles of mass m distributed over M hypercubic cells of size L^d. Each pair of particles contributes a negative amount $-\varepsilon$ to the total potential energy Φ if and only if they are in the same cell. When n_i is the number of particles in cell i, the total potential energy is

$$\Phi = -\tfrac{1}{2}\varepsilon \sum_{i=1}^{M} n_i(n_i - 1) \tag{2}$$

The nonextensive character of Φ without scaling of ε is obvious since Φ is proportional to N^2 for certain distributions $\{n_i\}$. After a straightforward integration over the momenta p_i the canonical partition function becomes $Z_c(N, V, T) = Q(N, V, T)/\lambda^{dN}$ with $\lambda = h/(2\pi m\beta^{-1})^{1/2}$, $\beta = 1/kT$, T the temperature, k Boltzmann's constant, and h Planck's constant. The spatial integrations appear in the configuration integral $Q(N, V, T)$ defined by

$$Q(N, V, T) = L^{dN} \sum_{\{n_i\}}{}' \frac{\exp \tfrac{1}{2}\beta\varepsilon(\sum_{i=1}^{M} n_i^2 - N)}{\prod_{i=1}^{M} n_i!} \tag{3}$$

where the prime in the summation indicates the constraint of particle conservation, $\sum_{i=1}^{M} n_i = N$. Note that the factorial $N!$ in the denominator of Z_c has canceled against the same factor in the number of possible combinations $N!/\prod_{i=1}^{M} n_i!$ over all cells for a given particle distribution. The free energy $F(N, V, T) = -\beta^{-1} \ln Z_c(N, V, T)$ is estimated by replacing

the summation over the possible distributions by the largest term. This can be justified for large N/M and M by bounding $\beta F/N$:

$$d\ln(\lambda/L) - \gamma_m - \ln \Upsilon/N \leqslant \beta F/N \leqslant d\ln(\lambda/L) - \gamma_m$$

with

$$\Upsilon = \binom{N+M}{M}$$

the number of terms in the constrained summation. The term γ_m is the maximum of

$$\gamma = -\frac{M}{2N}\ln(2\pi) + \frac{1}{2N}\sum_{i=1}^{M} \ln \nu_i + \frac{M}{2N}\ln N - \ln N + 1$$
$$+ \frac{1}{2}\beta\varepsilon\left(\sum_{i=1}^{M} N\nu_i^2 - 1\right) - \sum_{i=1}^{M} \nu_i \ln \nu_i \tag{4}$$

in the expression $Z_c = (L/\lambda)^{dN} \sum' \exp(N\gamma)$ when Stirling's approximation is used. In (4) the relative occupation number is defined as $\nu_i = n_i/N$. The first three terms in expression (4) are negligible for large N/M and M. Note that Eq. (4) is valid for $n_i \gg 1$.

The stationary points of γ or $\theta \equiv \gamma + \ln N - 1$ are calculated with respect to the constraints $\beta > 0$ and conservation of the total number of particles, which is restated as $\nu_M = 1 - \sum_{i=1}^{M-1} \nu_i$. From (4), they are found to be the solutions of

$$\beta\varepsilon N \nu_M = \frac{\ln(\nu_i/\nu_M)}{\nu_i/\nu_M - 1} \tag{5}$$

apart from the solution $\nu_i = 1/M$ for all i, which is always stationary. Equation (5) turns out to be the same stationarity condition as in the microcanonical ensemble once $\beta\varepsilon N$ is rewritten in terms of the energy parameter $\eta = 2\bar{E}/\varepsilon N^2 - 1/N$ [using the definition $\bar{E} = -(1/Z_c)\,\partial Z_c/\partial\beta$ and the maximum term approximation]:

$$\beta\varepsilon N = \frac{d}{\eta + \sum_{i=1}^{M} \nu_i^2} \tag{6}$$

Of course, in the canonical ensemble the energy $\bar{E}$ is a statistical quantity and the temperature a fixed parameter, whereas in the microcanonical ensemble it is the other way around. Hereafter, the distinction between E and $\bar{E}$ follows from the context. Total collapse occurs for $\eta = -1$. The

monotonic decreasing character-of the RHS of relation (5) as a function of v_i/v_M provides the solutions $0 < v_1 = v_2 = \cdots = v_q < v_{q+1} = \cdots = v_M \leqslant 1$ for $0 \leqslant q \leqslant M-1$ after relabeling the cell numbers, since the LHS of Eq. (5) is constant. The stationary points of θ are maxima if the eigenvalues λ of the characteristic equation

$$\left| \frac{\partial^2 \theta}{\partial v_k \, \partial v_l} - \lambda I \right| = 0$$

with I the identity matrix are all negative. The quantities $s = \beta\varepsilon N - 1/v_M$, $c = 2s - \lambda$, $r = \beta\varepsilon N - 1/v_1$, $a = s + r - \lambda$, and $t = 0$ appearing as elements in the characteristic matrix are modifications of equivalent definitions [with $t \neq 0$ and replacement of β via Eq. (6)] for the microcanonical ensemble; see ref. 2. A maximum is obtained if and only if $q = M - 1$ and

$$\lambda = (M-1)\, s + r < 0 \tag{7}$$

Thus, the two remaining solutions constitute a homogeneous phase with $v_k = v_M$ and a cluster phase with $v_k < v_M$ for $k = 1, \ldots, M-1$.

It turns out that all the thermodynamic quantities in the canonical as well as the microcanonical ensemble are equivalent using relation (6) to express temperature in terms of energy or vice versa, but the energy or temperature intervals for which the homogeneous or cluster phase exist are different. The condition (7) for the canonical ensemble and the equivalent one for the microcanonical ensemble determine these intervals as a function of v_M, N, and M.

According to condition (7), the homogeneous phase exists for $T > T_h = \varepsilon N/kM$, which in terms of the energy is exactly the range in the microcanonical ensemble $\eta > \eta_h = (d-1)/M$. The free energy F_h in the homogeneous phase is

$$\beta F_h(N, V, T) = N\left(d \ln \frac{\lambda}{L} + \ln N - 1 - \theta_h \right) \tag{8}$$

with $\theta_h = \frac{1}{2}\beta\varepsilon(N/M - 1) + \ln M$. The temperature is given by

$$T = \frac{\varepsilon N}{kd}\left(\eta + \frac{1}{M} \right) \tag{9}$$

as follows from Eqs. (5) and (6) after substitution of $v_i = 1/M$. Two different definitions of pressure can be used, because the variation in the volume $V = ML^d$ can take place with either M or L fixed, giving p_M or p_L,

respectively. With M fixed, the ideal gas law results, while with L fixed, an interaction term is added:

$$p_M = -\left.\frac{\partial F}{\partial V}\right|_M = \frac{NkT}{V}, \qquad p_L = -\left.\frac{\partial F}{\partial V}\right|_L = \frac{NkT}{V} - \frac{\varepsilon N^2}{2MV}$$

The temperature in the cluster phase is derived from the stationarity condition (5) and relation (6) with $v = v_M$ and $v_i = (1-v)/(M-1)$. One finds

$$T = \frac{\varepsilon N}{k(M-1)} \frac{1-Mv}{\ln[(1-v)/(M-1)v]} = \frac{\varepsilon N}{kd}\left(\eta + \frac{1-2v+Mv^2}{M-1}\right) \tag{10}$$

The cluster phase exists if condition (7) is obeyed. Elimination of the temperature by using Eq. (5) yields

$$Mv(1-v)\ln\frac{(M-1)v}{1-v} - (Mv-1) < 0 \tag{11}$$

which is identical to the requirement of a positive specific heat, i.e., $\partial\eta/\partial T = (\partial\eta/\partial v)(\partial v/\partial T) > 0$, in the canonical ensemble. The resulting temperature range is $0 < T < T_c(\eta_2)$ as depicted in Fig. 1, where the relation between the reduced temperature $T^* \equiv dkT/2\varepsilon$ versus the energy parameter η is plotted along with the various transitions and hystereses. The corresponding energy range in the microcanonical ensemble lies between $-1 < \eta < \eta_c$ as shown in Fig. 1, η_c being the energy where the tangent of temperature as a function of energy becomes infinite. The requirement $\partial\eta/\partial v < 0$ gives the same energy range when the stationarity condition for the microcanonical ensemble

$$\eta = \frac{d(Mv-1)}{(M-1)\ln[(M-1)v/(1-v)]} - \frac{1-2v+Mv^2}{M-1} \tag{12}$$

is used. The free energy F_c in the cluster phase has the form

$$\frac{\beta F_c(N, V, T)}{N} = d\ln\frac{\lambda}{L} + \ln N - 1 - \theta_c \tag{13a}$$

with

$$\theta_c = -(1-v)\ln\frac{(1-v)}{M-1} - v\ln v + \frac{1}{2}\beta\varepsilon\left[\frac{N}{M-1}(1-2v+Mv^2) - 1\right] \tag{13b}$$

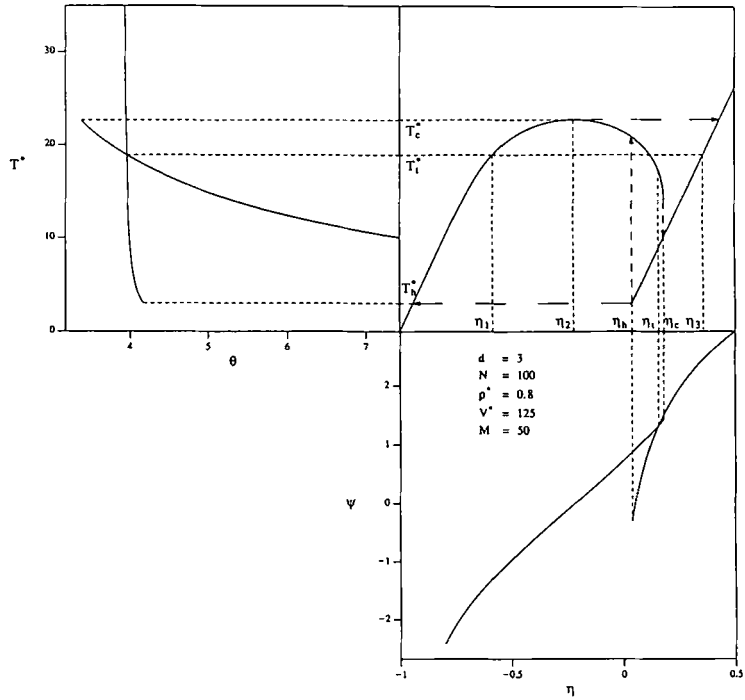

Fig. 1. Compound picture for the cell model of the reduced temperature $T^* = dkT/2\varepsilon$ versus the terms θ in the free energy which are dependent on the occupation number ν, and versus the energy parameter η. The quantity ψ in the entropy which depends on ν is also shown. The parameters are $N = 100$, $M = 50$, $d = 3$, $V^* = V/\sigma^d$, and $\rho^* \equiv N\sigma^d/V = 0.8$. Horizontal dashed lines with arrows at T_h^* and T_c^* indicate the hysteresis in the canonical ensemble. The vertical dashed lines with arrows at η_h and η_c show the hysteresis in the microcanonical ensemble. Phase transitions are defined to occur at intersections of the curves for θ and ψ in the homogeneous and cluster phases at temperature T_t^* and energy η_t in the canonical and microcanonical ensembles, respectively.

3. CANONICAL VERSUS MICROCANONICAL ENSEMBLE

The relations between temperature, energy, free energy, and entropy in Fig. 1 show the occurrence of hystereses and phase transitions in both the canonical and the microcanonical ensemble. The horizontal dashed lines (at T_h^* and T_c^*) and the vertical ones (at η_h and η_c) with arrows denote the hysteresis in the two ensembles. Phase transitions are assumed to occur when the free energies or entropies in the homogeneous and cluster phases are equal. The entropy[2] and free energy for large M and N/M are given by

$$\frac{S}{Nk}=\frac{1}{2}d\ln\left(\frac{2\pi m\varepsilon L^2}{\hbar^2 d}\right)+\left(\frac{1}{2}d-1\right)\ln N+\frac{1}{2}d+1$$
$$+\frac{1}{2}d\ln\left(\eta+\sum_{i=1}^{M}v_i^2\right)-\sum_{i=1}^{M}v_i\ln v_i \tag{14}$$

$$\frac{\beta F}{N}=d\ln\lambda+\ln\frac{N}{L^d}-\frac{1}{2}\beta\varepsilon\left(\sum_{i=1}^{M}Nv_i^2-1\right)+\sum_{i=1}^{M}v_i\ln v_i \tag{15}$$

The quantities

$$\theta=\tfrac{1}{2}\beta\varepsilon\left(\sum_{i=1}^{M}Nv_i^2-1\right)-\sum_{i=1}^{M}v_i\ln v_i \tag{16a}$$

$$\psi=\tfrac{1}{2}d\ln\left(\eta+\sum_{i=1}^{M}v_i^2\right)-\sum_{i=1}^{M}v_i\ln v_i \tag{16b}$$

represent the terms in the free energy and entropy, respectively, that vary with respect to temperature and energy, respectively, as well as with the relative occupation number. Equation (16b) appeared in the earlier publication.[2] The phase transition temperature in the canonical ensemble is denoted by T_t and the transition energy in the microcanonical ensemble by η_t. The region $\eta_2 \leqslant \eta \leqslant \eta_c$ of negative specific heat found to exist in the microcanonical ensemble is by definition excluded in the canonical ensemble, for which the surrounding heat bath bridges the region with a constant-temperature phase transition.

There is another way to consider the stationary points of the entropy or free energy of the cell model. The free energy is given as a function of T and v. Minimization of the free energy with respect to T is possible by considering $v=v(T)$, a relation implicit in the stationarity condition (5). Two minima will arise: one corresponding to the homogeneous phase and one to the cluster phase. For temperatures $T<T_t$ the cluster solution belongs to the absolute minimum of F, implying that for the interval $T_h<T<T_t$ the cluster phase is metastable, and for $T_t<T<T_c$ the homogeneous phase is metastable. The same kind of reasoning is valid for entropy maximization in the microcanonical ensemble, resulting in metastable states for homogeneous and cluster phases in the intervals $\eta_t<\eta<\eta_c$ and $\eta_h<\eta<\eta_t$, respectively.

A Maxwell construction[1] graphically elucidates the relationship between both ensembles. Conservation of entropy $\Delta S=\Delta E/kT$ yields

$$\int_{\eta_1}^{\eta_3}\frac{d\eta}{T(\eta)}=\frac{\eta_3-\eta_1}{T_t} \tag{17}$$

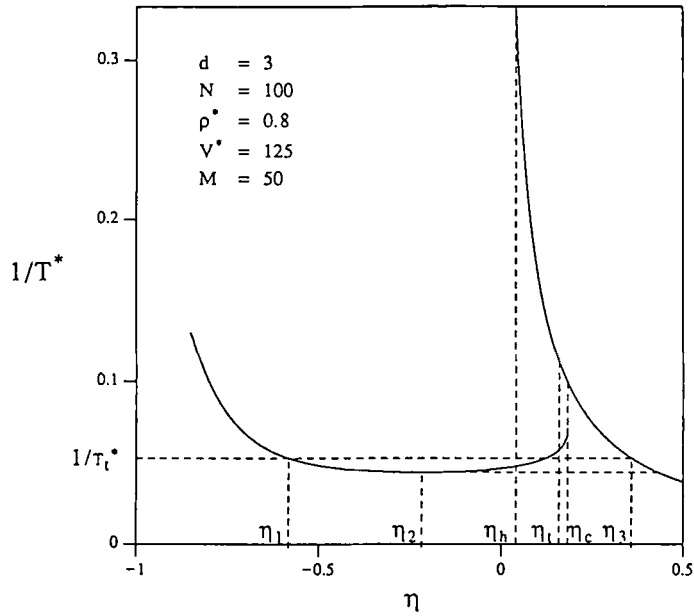

Fig. 2. Inverse reduced temperature $1/T^*$ versus energy η. The entropy change between η_1 and η_3 in both ensembles is equal. The Maxwell construction ensures that the areas between the theoretical curves and $1/T_t^*$ below and above that value are equal, where it is understood that the cluster phase ends and the homogeneous phase starts at η_t.

The changes in entropy in both ensembles are equal: Figure 2, depicting the inverse temperature versus the energy parameter η, shows that the areas between the theoretical curves and the transition temperature $1/T_t^*$ below and above that value are the same for the microcanonical cluster and homogeneous phases for $-1 < \eta < \eta_t$ and $\eta_t < \eta$, respectively.

The large-system behavior can be approached in terms of different scaling procedures, indicated by I and II. Procedure I, used by Hertel and Thirring,[1] restores the extensivity in the cell model by taking εN, V/N, E/N, and $M = V/L^d$ as constant for $N \to \infty$, leading to the usual way thermodynamics is found from statistical mechanics. The scaling is similar to a mean-field approach for a van der Waals gas. In this limit the thermodynamic quantities remain a function of the cell number M, the length L of the hypercube increases to infinity, and the depth of the potential reduces to zero. The first two cumbersome terms in the entropy and free energy written in Eqs. (14) and (15), respectively, combine to finite quantities in the appropriate thermodynamic limit. The minimum temperature

in the homogeneous phase is $T_h^I = (\varepsilon N)_\infty^I/(Mk)$ and the corresponding energy is $\eta_h^I = (d-1)/M$, which is constant in the limit.

This procedure is perfectly sound from a mathematical point of view. However, the remaining dependence on M and the behavior of L as $N^{1/d}$ are artificial from a physical point of view, and so is the scaling of ε with $1/N$. Due to these features, the procedure cannot be used to obtain from the cell model an estimate of the asymptotic properties of systems with the true pair potential of Eq. (1), all having identical values of σ and ε but different values of $V = N\sigma^d$ and $E = N\varepsilon$.

Therefore, a second procedure, II, has been proposed[2]: $N \to \infty$ with L, V/N, and M/N constant, and with E/N or T constant for respectively the microcanonical or the canonical ensemble. In this procedure the nonextensive character of the cell model is maintained, and the thermodynamic limit does not exist. A third procedure is to let $N \to \infty$ with L, V/N, M/N, and E/N^2 constant. This would differ from a rescaled version of I in having the number of cells grow with system size.

It is our belief that II, where the energy only grows with N, is relevant for our universe. We think that II makes the cell model interesting from a cosmological point of view, even though it provides only the crudest approximation to the true gravitational potential. It is not so strange to conclude that an essential dependence of detailed properties of the system on its size, however large, reflects a basic property of the actual universe, even though the cell model completely neglects the singularity and the long range of the true gravitational potential.

Only the main results obtained, in particular from Eqs. (7) and (12), with procedure II will be given here, postponing a further discussion to a later paper. It is found that in the canonical ensemble, at finite temperatures, only the completely collapsed state survives when the system becomes larger and larger; in particular, all homogeneous states become increasingly metastable. In contrast, in the microcanonical ensemble for larger and larger systems it is only the region around $\eta = 0$ that is relevant. At $\eta = 0$ the number of particles in the collapsing cluster is asymptotically given by $n_M = dN/\ln M$, whereas the homogeneous background approaches the constant density N/M. In this situation, transient nonequilibrium states with (many) more than one collapsing cluster are expected to become more and more important. The appearance of logarithmic quantities is typical for the nonextensive behavior. The entropy surface becomes extremely flat, indicating divergent relaxation times: in fact, the maximum-term method as applied to Eq. (4) is found to degenerate.

The Hertel and Thirring cell model seems to be most useful and physically sound in the microcanonical ensemble in procedure II for a large but finite amount of particles. It tries to mimic the basic instabilities due to the

gravitational potential for systems that are not easily put into a heat bath. For large N, with procedure II dictating the behavior of the other independent variables, the cell model tends to be in the metastable region at $\eta \approx 0$ (to avoid this region one would have to assume that E behaves asymptotically as N^2), which becomes a critical point of the system. The fluctuations of the cluster size in the associated pair-potential models will also appear to be quite large. Our expectation that large systems with purely attractive potentials are likely to be trapped in a critical state of many clusters in a homogeneous background corresponds qualitatively with the situation found in the universe. Large fluctuations with long lifetimes are to be expected for gravitational systems in nonequilibrium states.

4. ONE-DIMENSIONAL COLLAPSING SYSTEM

Consider a one-dimensional model with N particles of mass m with coordinates $x_1, x_2, ..., x_N$ and momenta $p_1, p_2, ..., p_N$ in a volume of length l. The discrete pair potential

$$\phi(r) = \begin{cases} 0 & \text{if } r \geqslant \sigma \\ -\varepsilon & \text{otherwise} \end{cases} \tag{18}$$

is a rewritten version of the potential (1) for $\delta \to \infty$: it is a rectangular well of depth $-\varepsilon$ and width σ. The total potential energy Φ is

$$\Phi = \sum_{i<j}^{N} \phi(r_{ij})$$

with $r_{ij} = |x_i - x_j|$, and the kinetic energy is $E_{\text{kin}} = \sum_{i=1}^{N} p_i^2/2m$. Exact solutions for $N = 2, 3, 4$ are readily found for this one-dimensional model, both for periodic and nonperiodic boundary conditions.

Simulations of the one-dimensional particle model are based on the method due to Alder and Wainwright[6] for molecular dynamics of systems with discrete pair potentials. The numerical method distinguishes among the three different collisions involved. A collision is defined to occur when the distance between a pair of particles becomes equal to σ. The three types of collisions are: a bounce, in which two particles do not have enough kinetic energy to cross the potential barrier of $-\varepsilon$, which therefore acts as a solid wall; dissociation, in which two particles escape their mutual potential well with less kinetic energy than before the collision; and capture, two particles experience their attraction by a push towards each other. Changes in speed and kinetic energy after a collision are calculated from the conser-

vation of momentum and energy per pair of colliding particles. Upcoming collision events are handled in time by using an ordered list of collision times. The overhead involved in maintaining the list of collision times is reduced ingeniously,[6] decreasing the computation time drastically. A comparison with the cell model is achieved by equating $L \equiv 2\sigma$, taking the cell size twice as large as σ [for $\delta \to \infty$, the inflection point of Eq. (1) occurs at $r = \sigma$]. The simulations are performed with periodic boundary conditions on both a minicomputer (μDutch) and on a workstation (Silicon Graphics), the latter being about 40 times faster than the former. The runs are taken in sequences of increasing ("heating") or of decreasing energy ("cooling"), or independent of one another with random or ordered initial conditions. In the first case of a series of coupled runs the final configuration (positions and velocities) of a run is the initial configuration for the next run. The kinetic energy is rescaled in that process such as to accom-

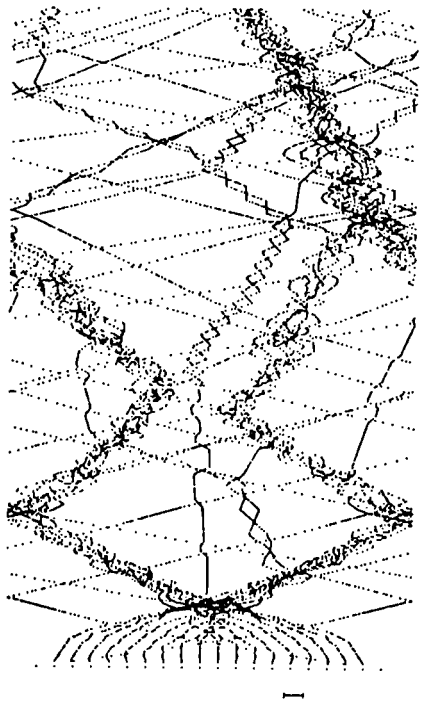

Fig. 3. The trajectories of $N = 20$ particles with a square-well pair potential ($\eta = 0.1$, $\rho^* = 0.95$). The line segment below indicates the potential width. The particles start in a slightly distorted motionless row except for the outermost particles, which have opposite velocities. Each configuration, depicted horizontally, is separated by 40 collisions.

modate a higher or lower-total energy. The procedure decreases the total equilibration time considerably if the increments or decrements of the energy are not too large. The initialization of the first run in a sequence or a separate simulation is chosen to be either random or a slightly distorted row with all particles motionless except the two outermost particles. The distortion of the row avoids the occurrence of exactly equal collision times excluded in the numerical algorithm for practical reasons. As an example, the time development of 20 particles with the pair potential of Eq. (18) is given in Fig. 3. For 100 configurations, each separated by 40 collisions, the positions (horizontal) are plotted as a function of time (vertical).

Measurements of temperature, pressure, cluster size, and specific heat are taken after an equilibration time, determined by the disappearance of drifts in the kinetic energy amid the existent fluctuations. In Fig. 4, a plot of the (reduced) kinetic energy E^*_{kin} versus the time, equilibration is achieved after 5000 (dimensionless) time units. The pressure p is determined by a method of Hoover and Alder.[7] The specific heat C_V is calculated using an approach developed by Lebowitz *et al.*[8] The relative occupation number $\nu \equiv (N_c/N)$ in the numerical experiments, based on the amount of particles N_c in a cluster, is determined using an algorithm of

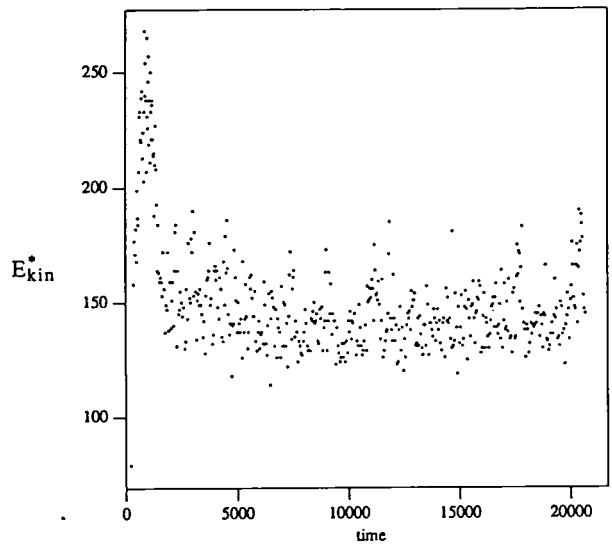

Fig. 4. Reduced kinetic energy E^*_{kin} versus time of simulations with $N = 60$, $\eta = 0.0259$, $\rho^* = 0.8$. Equilibration is achieved at (dimensionless) times > 5000. The first peak corresponds to the formation of a cluster, which is initially rather "warm." The other peaks correspond to typical collective oscillations of the cluster.

Stoddard.[9] Defining a critical radius r_c, two particles belong to the same cluster if their interparticle distance is less than r_c given the constraint that each particle is part of only one cluster at a time. Therefore, a cluster of particles might have the appearance of a chain, which accounts for the overestimation of the actual cluster size in the homogeneous phase. The following dimensionless quantities are introduced for computational convenience:

$$E^*_{\text{kin}} = \frac{E_{\text{kin}}}{\varepsilon}, \qquad T^* = \frac{dkT}{2\varepsilon}, \qquad \rho^* = \frac{N\sigma^d}{V}$$

5. SIMULATIONS AND CELL MODEL

The simulations with the rectangular-well pair potential are in closer correspondence to the solution of the cell model than simulations[2,5] with smooth pair potentials, with lower values of δ (see the discussion in the appendix of ref. 2 of the independent-particle model as a description for the completely collapsed state). A plot of T^* versus η reveals the agreement between cell model (solid and dashed lines) and simulations for $N = 60$ and $N = 120$ for $\rho^* = 0.8$ in Figs. 5a and 5b. It should be realized that the cell model is solved provided N/M and M are large, while the number of particles in the simulations above is quite small. Nevertheless, the similarities are striking. The open circles and squares in Fig. 5a denote a sequence of measurements in a heating and cooling series, respectively. Insufficient equilibration times for $-0.3 < \eta < 0.1$ caused the large difference between cell model and measurements as well as the fluctuations in the data during the heating sequence. Longer equilibration times were used in the cooling sequence: the squares lie closer to the predicted curve for the cell model and the region of negative specific heat exists. Closed circles indicate results obtained in much longer separate runs. The simulations in Fig. 5b for $N = 120$ particles confirm the agreement for cooling sequences with longer equilibration times. Fluctuations are intrinsic in the cluster phase, especially in the region of negative specific heat, where the kinetic energy exhibits large wavelike fluctuations ($\sim 30\%$) and longer periods are required to provide adequate statistics for the measurements. The insufficient computation time is apparent in the slight scatter in the cluster phase in Fig. 5b. The temperature in the cell model and in the true pair-potential model are equal for $\eta \approx -1$, where $T^* \approx \frac{1}{2}N(\eta + 1)\delta/(\delta + 2)$, which for $\delta \to \infty$ is equal to $\frac{1}{2}N(\eta + 1)$; see the appendix of ref. 2. At $\eta \approx -1$, the system is in the state of complete collapse where the amount of kinetic energy is too small to break any of the $\frac{1}{2}N(N-1)$ bonds between the particles. In the homogeneous phase one has $T^* = \frac{1}{2}N(\eta + \eta_0)$, with

$\eta_0 = 1/N$ assuming ideal gas behavior and $\eta_0 = 1/M$ for the cell model. The equivalence close to the ground state and in the homogeneous phase between the simulations and the cell model explains the better agreement relative to former simulations at lower values of δ; there is not much freedom left for large deviations at intermediate energies. The relative

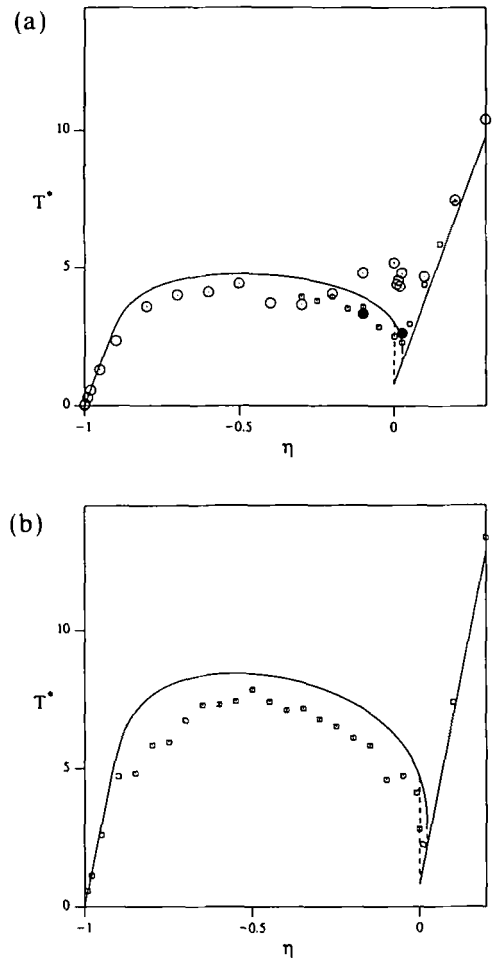

Fig. 5. Temperature T^* versus energy η with $\rho^* = 0.8$ for the cell model (solid lines; the dashed lines indicate the metastable transitions) and as observed in the simulations (circles and squares). Apart from the length scale $L = 2\sigma$ there are no adjustable parameters. (a) $N = 60$. Open circles denote a heating and squares a cooling sequence. Closed circles are separate measurements. (b) $N = 120$. Measurements in a cooling sequence.

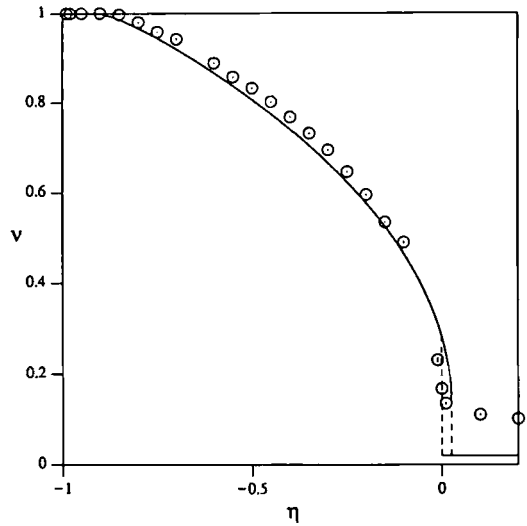

Fig. 6. The relative occupation number ν of the cluster for the cell model (solid and dashed lines) and the simulations with $N = 60$, $\rho^* = 0.6$.

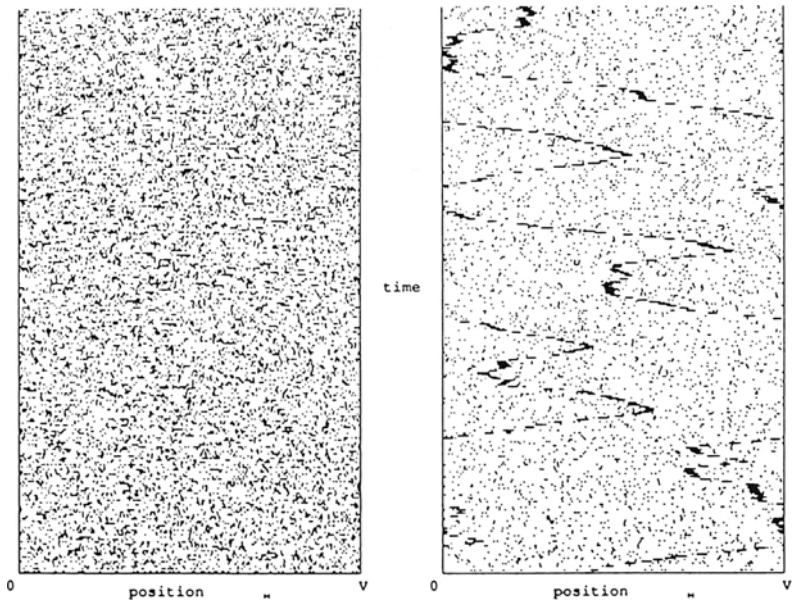

Fig. 7. Position–time plots for $N = 60$, $\rho^* = 0.8$. A total of 300 configurations is plotted horizontally every 12,000 collisions. The width of the square well is indicated by the line segments below the figures. (a) The system is in the homogeneous phase, $\eta = 0.01$. (b) The system is in the cluster phase, $\eta = -0.3$, $\nu = 0.7$ (the specific heat is negative). Both simulations are part of the cooling event in Fig. 5a.

occupation number ν of the cluster is plotted in Fig. 6 for 60 particles and $\rho^* = 0.6$. Deviations of ν between cell model and simulation in the homogeneous phase originate in the systematic overestimation of the cluster size inherent to the use of Stoddard's algorithm.[9] Specific heat and pressure show the same behavior with larger fluctuations, because these indirectly measured quantities require more computation. The phase transition and the movement of the cluster are clearly visible in the position–time plots of Fig. 7 for $N = 60$, $\rho^* = 0.8$, (a) $\eta = 0.01$ just in the homogeneous phase, and (b) $\eta = -0.3$, $\nu = 0.7$ in the cluster phase. A total of 300 configurations is plotted horizontally, separated vertically, in time, by 12,000 collisions. The degree of grayness is a measure for the density. The line segment underneath the horizontal position axis denotes the width σ of the potential well. The variation in the kinetic energy is shown in Fig. 8 for $N = 60$, $\rho^* = 0.8$, $\eta = -0.4$, $\nu = 0.77$ as a function of time in

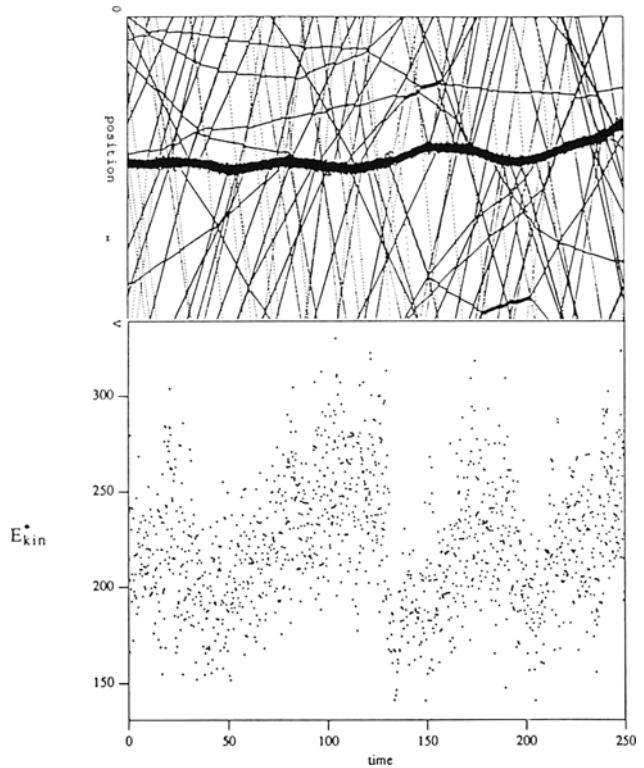

Fig. 8. Variation of kinetic energy E^*_{kin} as a function of time and the corresponding position–time plot for $N = 60$, $\rho^* = 0.8$, $\eta = -0.4$, $\nu = 0.77$. The simulation is part of the heating event in Fig. 5a.

combination with the corresponding position–time diagram. A drop in kinetic energy indicates the breaking of interparticle bonds. The rather large fluctuations are a typical feature of these unstable systems; they are due to collective cluster modes.

6. CONCLUDING REMARKS

The simulations of the one-dimensional model with the rectangular-well pair potential described in this paper agree even better with the cell model than earlier simulations with smooth, purely attractive short-range potentials, due to the similarity of the two models near the ground state.

It would be worthwhile to compare the solution of the cell model with an analytical solution of the one-dimensional model with a rectangular-well pair potential, which would elucidate the differences for systems that are too large for simulation. Analytical studies of this one-dimensional model are in progress.

The Hertel and Thirring cell model is one of the few analytically tractable models for unstable systems in arbitrary dimensions, both in the canonical and the microcanonical ensemble. Two scaling procedures in the thermodynamic limit have been discussed. In the first scaling procedure, the cell size and the range of the purely attractive pair potentials are adjusted to ensure the extensivity of the model in the cluster phase, which thus becomes an ordinary statistical mechanical model. In the second scaling procedure cell size and range are kept fixed on physical grounds. It leads to rather unusual nonextensive behavior in the cluster phase. For $N \to \infty$, complete collapse at $\eta \approx -1$ is the only state that survives in the canonical ensemble. More interesting for us is the microcanonical ensemble, with procedure II, in which large systems are most likely found in the critical state at $\eta \approx 0$. Due to its nonextensivity and large fluctuations this state exhibits a certain cosmological appeal.

ACKNOWLEDGMENTS

The authors are indebted to Y. Fonk, J. Heringa, H. A. Posch, H. Narnhofer, and W. Thirring for stimulating discussions, and to the latter three also for a videotape showing the behavior of collapsing systems.

REFERENCES

1. P. Hertel and W. Thirring, A soluble model for a system with negative specific heat, *Ann. Phys.* (N.Y.) **63**:520 (1971).
2. A. Compagner, C. Bruin, and A. Roelse, Collapsing systems, *Phys. Rev. A* **39**:5089 (1989).

3. M. K. H. Kiessling, On the equilibrium statistical mechanics of isothermal classical self-gravitating matter, *J. Stat. Phys.* **55**:203 (1989).
4. H. A. Posch, H. Narnhofer, and W. Thirring, Dynamics of unstable systems, *Phys. Rev. A* **42**:1880 (1990); Externally perturbed systems, *J. Stat. Phys.* **65**:555 (1991).
5. H. A. Posch, H. Narnhofer, and W. Thirring, *Simulation of Complex Flows*, M. Mareschal, ed. (Plenum Press, New York, 1990), p. 291.
6. B. J. Alder and T. E. Wainwright, Studies in molecular dynamics. I. General method, *J. Chem. Phys.* **31**(2):459 (1959).
7. W. G. Hoover and B. J. Alder, Studies in molecular dynamics. IV. The pressure, collision rate, and their number dependence for hard disks, *J. Chem. Phys.* **46**(2):486 (1967).
8. J. L. Lebowitz, J. K. Percus, and L. Verlet, Ensemble dependence of fluctuations with applications to machine computations, *Phys. Rev.* **153**:250 (1967).
9. S. D. Stoddard, Identifying clusters in computer experiments on systems of particles, *J. Comp. Phys.* **27**:291 (1978).